JCB Article

Presenilin 1 mediates the turnover of telencephalin in hippocampal neurons via an autophagic degradative pathway

Cary Esselens,[1] Viola Oorschot,[3] Veerle Baert,[1] Tim Raemaekers,[1] Kurt Spittaels,[4] Lutgarde Serneels,[2] Hui Zheng,[6] Paul Saftig,[5] Bart De Strooper,[2] Judith Klumperman,[3] and Wim Annaert[1]

[1]Membrane Trafficking Laboratory and [2]Neuronal Cell Biology and Gene Transfer Laboratory, Center for Human Genetics/ VIB04, KULeuven, 3000 Leuven, Belgium
[3]Department of Cell Biology, University Medical Center Utrecht, 3584CX Utrecht, Netherlands
[4]Galapagos Genomics, B-2800 Mechelen, Belgium
[5]Institute of Biochemistry, University of Kiel, D-24118 Kiel, Germany
[6]Division of Neuroscience, Baylor College of Medicine, Houston, TX 77030

Presenilin 1 (PS1) interacts with telencephalin (TLN) and the amyloid precursor protein via their transmembrane domain (Annaert, W.G., C. Esselens, V. Baert, C. Boeve, G. Snellings, P. Cupers, K. Craessaerts, and B. De Strooper. 2001. *Neuron*. 32:579–589). Here, we demonstrate that TLN is not a substrate for γ-secretase cleavage, but displays a prolonged half-life in PS1$^{-/-}$ hippocampal neurons. TLN accumulates in intracellular structures bearing characteristics of autophagic vacuoles including the presence of Apg12p and LC3. Importantly, the TLN accumulations are suppressed by adenoviral expression of wild-type, FAD-linked and D257A mutant PS1, indicating that this phenotype is independent from γ-secretase activity. Cathepsin D deficiency also results in the localization of TLN to autophagic vacuoles. TLN mediates the uptake of microbeads concomitant with actin and PIP2 recruitment, indicating a phagocytic origin of TLN accumulations. Absence of endosomal/lysosomal proteins suggests that the TLN-positive vacuoles fail to fuse with endosomes/lysosomes, preventing their acidification and further degradation. Collectively, PS1 deficiency affects in a γ-secretase–independent fashion the turnover of TLN through autophagic vacuoles, most likely by an impaired capability to fuse with lysosomes.

Introduction

Presenilin 1 and 2 (PS1/2) play a catalytic role in the γ-secretase complex needed for regulated intramembrane proteolysis of the amyloid precursor protein (APP; for review see Annaert and De Strooper, 2002; Selkoe and Kopan, 2003). This event results in the final liberation of the amyloid β (Aβ) peptide. For its activity it requires the coordinated action of essential components including nicastrin, pen-2, and aph1. These proteins incorporate into a high molecular weight complex and depend on each other for their maturation, endoproteolysis, and stability (for review see De Strooper, 2003). The aspartate 257 and 385 (amino acid numbering of human PS1) most probably form the catalytic core of this complex (Wolfe et al., 1999). Next to APP, the γ-secretase complex is responsible for intramembrane proteolysis of a growing list of type I integral membrane proteins (for review see Annaert and De Strooper, 2002; Selkoe and Kopan, 2003). This mediates a multitude of downstream signaling cascades, either by generating an intracellular domain that acts as a transcriptional (co)factor or by regulating the availability of associated protein networks.

Next to γ-secretase cleavage, PSs are implicated in at least two other pathways. Koo and coworkers demonstrated that PS1 is a negative regulator of the Wnt/β-catenin signaling pathway mediating the degradation of β-catenin indepen-

The online version of this article includes supplemental material.

Address correspondence to Wim Annaert, Membrane Trafficking Laboratory, CME-VIB04, Gasthuisberg-KULeuven, 3000 Leuven, Belgium. Tel.: (32) 16-346371. Fax: (32) 16-347181.
email: Willem.Annaert@med.kuleuven.ac.be

Key words: autophagic vacuole; hippocampal neuron; phagocytosis; presenilin 1; telencephalin

Abbreviations used in this paper: APP, amyloid precursor protein; CatD, cathepsin D; CTF, COOH-terminal fragment; EndoH, endoglycosidase H; MDC, monodansylcadaverine; MOI, multiplicity of infection; PIP2, phosphatidylinositol 4,5 bisphosphate; PS, presenilin; SFV, Semliki Forest virus; TLN, telencephalin.

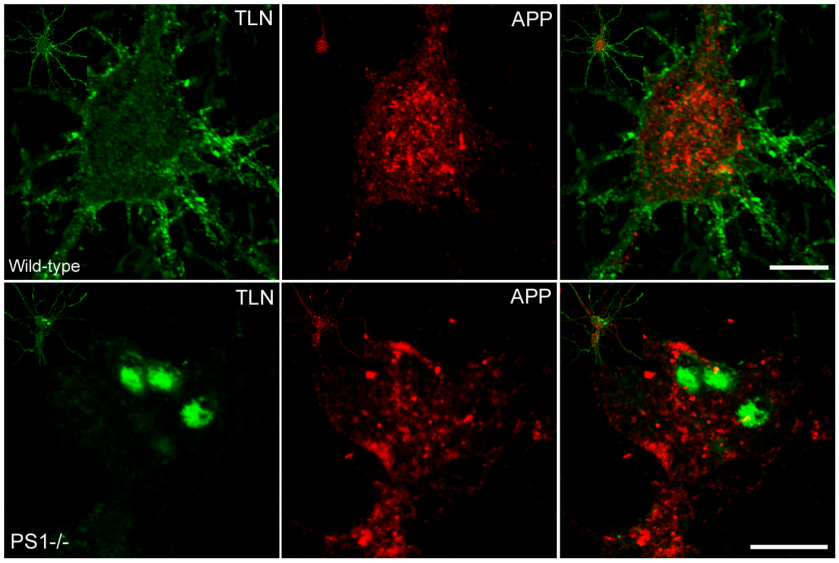

Figure 1. **Full-length TLN (but not APP) accumulates in a distinct compartment in PS1$^{-/-}$ hippocampal neurons.** Double-immunofluorescence staining for endogenous TLN (green, B36.1) and APP (red, mAb C1 6.1) in wild-type (top) and PS1$^{-/-}$ (bottom) hippocampal neurons (15-d culture). The inset shows an overview of the neuron. In wild-type neurons TLN labeling is essentially localized to the somatodendritic plasmalemma in contrast to APP, which is found in intracellular compartments. In addition, PS1 deficiency causes TLN, but not APP, to cluster in large somatic accumulations. Bars, 10 μm.

dent from the Axin/CK1α route (Kang et al., 2002). Second, PSs modulate capacitative calcium entry, a refilling mechanism for depleted intracellular calcium stores (Yoo et al., 2000). Furthermore, PS1 may regulate the trafficking of selected transmembrane proteins such as TrkB (Naruse et al., 1998), but also APP (Cai et al., 2003; Kaether et al., 2002) and nicastrin (for review see De Strooper, 2003). From these analyses it was suggested that PS1 modulates the trafficking in the early secretory pathway or during internalization at the cell surface, but in most cases this could not be clearly dissociated from its stabilizing or catalytic role in γ-secretase. The molecular basis for a trafficking role of PS1 is still far from being elucidated.

We documented before (Annaert et al., 2001) the interaction of PS1with telencephalin (TLN), a neuron-specific intercellular adhesion molecule (ICAM-5; Gahmberg, 1997) involved in dendritic outgrowth (Tian et al., 2000) and long-term potentiation (Nakamura et al., 2001). As for APP, the interaction is mediated through the PS1 COOH terminus and the first transmembrane domain, which may form a binding pocket with the transmembrane region of TLN. These findings have led us to propose a ring structure topology for PS1 in which the catalytic and substrate-binding site are spatially separated (Annaert et al., 2001). In PS1$^{-/-}$ hippocampal neurons, TLN accumulates in large somatic structures, coupling PS1 function to TLN localization and trafficking. However, both the nature of these accumulations as well as the question whether they originate as a direct consequence of impaired γ-secretase processing of TLN remained unsolved.

Using independent approaches, we now demonstrate that TLN is not a regulated intramembrane proteolysis substrate. We confirm that its accumulation in PS1-deficient neurons is not modulated by γ-secretase inhibitors and can be rescued by adenoviral expression of wild-type, FAD-linked and D257A mutant PS1. In fact, full-length TLN displays a delayed turnover and accumulates in an intracellular compartment in the absence of PS1. Here, we demonstrate that this compartment displays several features reminiscent of autophagic vacuoles. Autophagy is one of the major pathways of degradation of intracellular proteins. It thereby contributes to the balance between protein synthesis and degradation, which is essential in the control of growth and metabolism of cells. Autophagic vacuole formation in neurons is poorly understood, and it has been suggested that it may play a temporary protective role in early stages of apoptosis or even delay apoptosis (Jellinger and Stadelmann, 2000). Interestingly, the TLN accumulations are not acidified and do not acquire endosomal/lysosomal components, suggesting a failure of lysosomal fusion. Finally, we propose a phagocytic origin of these accumulations based on the microbead uptake experiments in neurons. Together, our data link PS1 to an autophagic degradative route distinct from its γ-secretase function.

Results

TLN is not cleaved by γ-secretase

In wild-type hippocampal neurons, TLN localizes to the plasmalemma, whereas in 30% of PS1$^{-/-}$ neurons, TLN additionally accumulates in large somatic structures (Fig. 1), the identity of which remained elusive (Annaert et al., 2001). To our surprise, APP, a substrate for γ-secretase, did not coenrich in these structures, suggesting that PS1 deficiency affects APP and TLN differentially. Therefore, we tested whether TLN is a γ-secretase substrate. In 15-d-old PS1$^{-/-}$ hippocampal cultures we could not detect any TLN COOH-terminal fragment (CTF), as opposed to APP-CTF, which readily accumulates (Fig. 2 A). Even upon Semliki Forest virus (SFV)–induced overexpression, no TLN-CTF was detected. Because no putative mechanism of shedding of the TLN ectodomain is known, we generated a TLNΔE that could serve as a potential γ-secretase substrate. However, no intracellular domain fragments were detected, indicating the absence of γ-secretase cleavage. Because this could reflect a fast turnover of the intracellular domain after cleavage, as seen for Notch and APP, we used a highly sensitive reporter assay (Struhl and Adachi, 2000) by coupling the Gal4VP16 transactivator to the cytoplasmic domain of TLN. Release

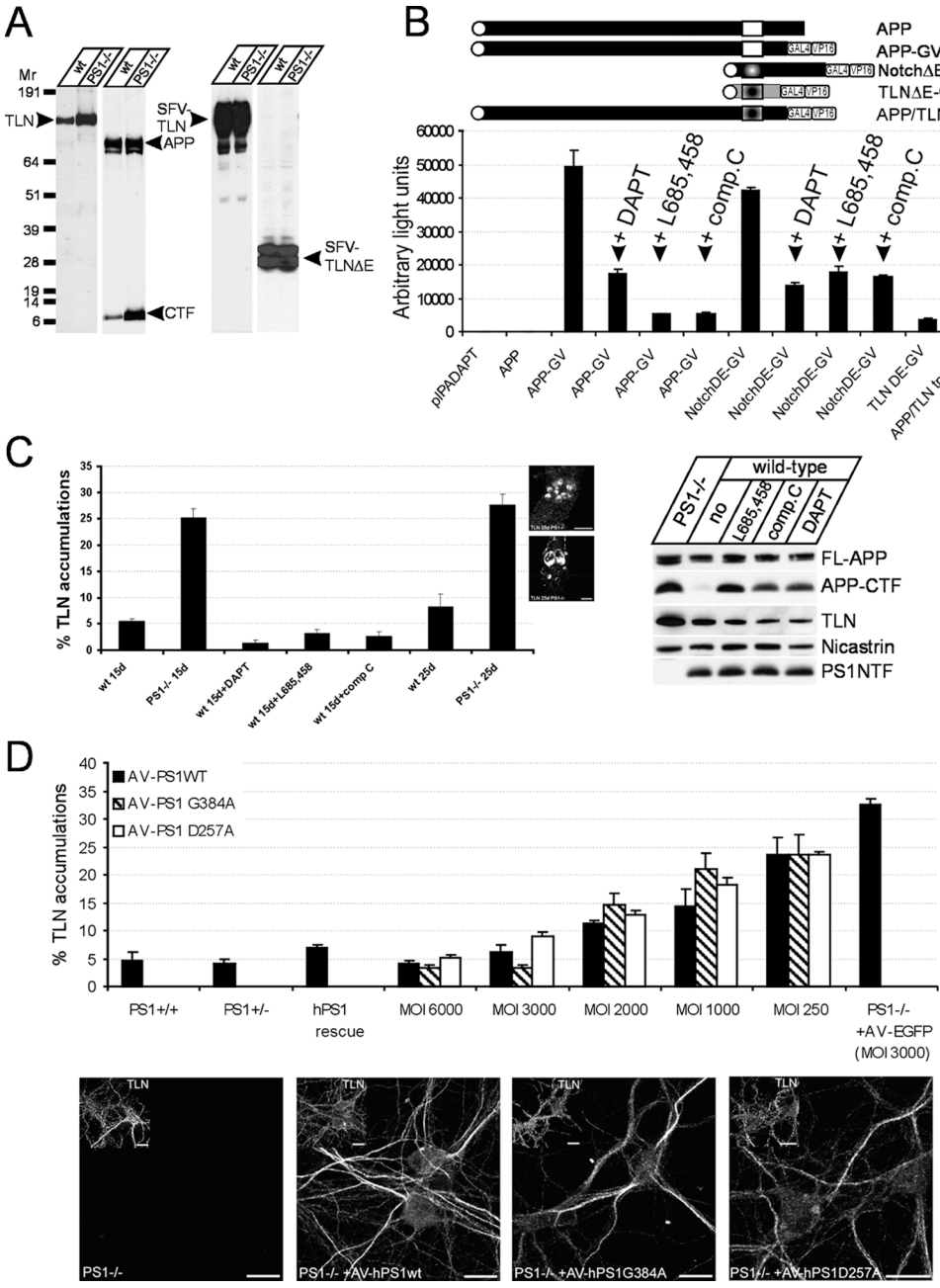

Figure 2. **TLN lacks the characteristics of a γ-secretase substrate.** (A) Western blot analysis of endogenous TLN and APP in wild-type and PS1$^{-/-}$ hippocampal neurons. PS1 deficiency results in the accumulation of APP-CTF. No TLN-CTF (estimated ± 7 kD) was detected, neither was it detected after SFV-induced exogenous overexpression. Also, overexpression of a TLNΔE fragment did not generate a PS1-dependent TLN intracellular domain. (B) Different constructs fused to the Gal4VP16 domain were used in a γ-secretase reporter assay. Control transfections (pIPspAdApt empty vector and pIPspAdApt-APP without Gal4VP16) show no luciferase activity. APP-Gal4VP16 and NotchΔE-Gal4VP16 activate the luciferase gene upon cleavage and are inhibited by DAPT, L658,458, or compound 32 (125 nM). No luciferase activity was detected using TLNΔE or APP in which the transmembrane domain was replaced by that of TLN (APP/TLN$_{TMR}$ chimaera), indicating that this region is not cleaved by γ-secretase. (C) Left: γ-secretase inhibitors do not induce the formation of TLN accumulations. Wild-type hippocampal neurons were treated with γ-secretase inhibitors (125 nM, daily from d 7–14 post-plating), fixed, and immunostained for TLN and the percentage of neurons with TLN accumulations was scored. Culturing neurons for 25 d increases the size and number (insets), but not the frequency of TLN accumulations (mean ± SEM, $n = 3$, 200–700 neurons per time point). Right: Western blot showing that only APP-CTF accumulates after chronic treatment with γ-secretase inhibitors. (D) Adenoviral reintroduction of human PS1 suppresses TLN accumulations. 30–35% of PS1$^{-/-}$ neurons display TLN accumulations, in contrast to <5% in PS1$^{+/+}$ and $^{+/-}$ cultures as well as in cultures expressing human PS1 in a PS1$^{-/-}$ background. However, suppression of TLN accumulations was obtained by adenoviral introduction of human PS1. A clear dose-dependent inhibition was seen with increasing MOI of adenoviral (AV) human PS1, but also the familial Alzheimer's disease-linked PS1G384A and dominant-negative PS1D257A mutants. Control adenoviral infections with eGFP did not have a significant effect. After 9–11 d post-infection (15 d post-plating), neurons displayed significant PS1 protein expression as demonstrated by double staining for TLN and human PS1(mAb 5.2). Bars, 20 μm.

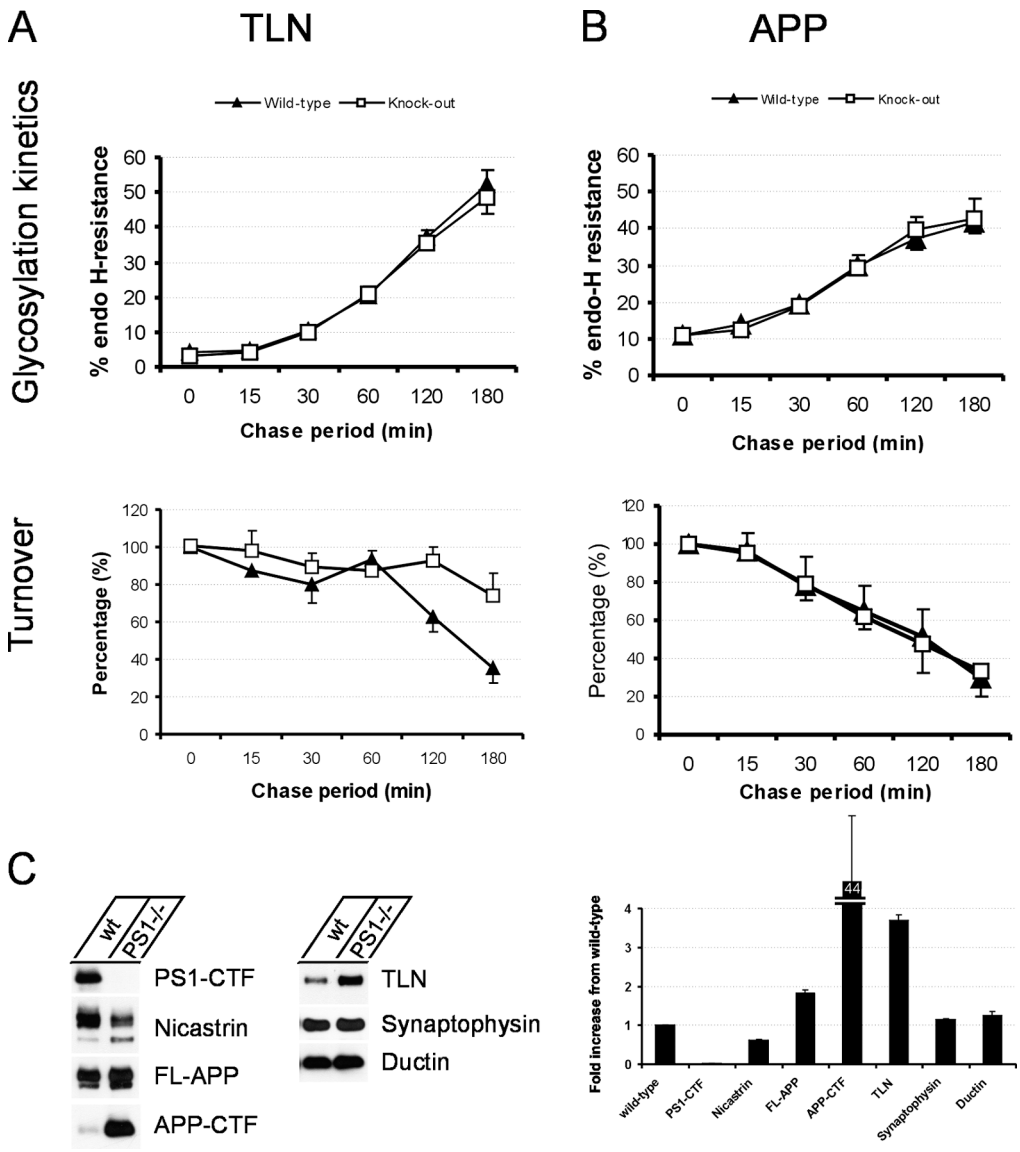

Figure 3. **Turnover of full-length TLN is altered in PS1$^{-/-}$ neurons.** Wild-type and PS1$^{-/-}$ cortical neurons were transduced with SFV-TLN (A) or -APP (B), pulse labeled for 15 min with [^{35}S]methionine, and chased for different time periods. Immunoprecipitated TLN and APP were treated with EndoH and analyzed by SDS-PAGE and phosphorimaging. The accumulation of an EndoH-resistant band indicates progressive maturation during Golgi passage; however, the ratio of EndoH-resistant to -sensitive TLN (A, top) and APP (B, top) revealed no difference (mean ± SEM, $n = 3$). Instead, the half-life of overexpressed TLN (A, bottom), but not full-length APP (B, bottom), is significantly prolonged in PS1$^{-/-}$ neurons (mean ± SEM, $n = 3$). (C) Wild-type and PS1$^{-/-}$ hippocampal neurons (12 d) were scraped, pelleted, and treated with 10 mU EndoH, followed by Western blot detection of APP, TLN, PS1, nicastrin (NCT), synaptophysin, and ductin. TLN levels are increased almost fourfold in PS1$^{-/-}$ neurons. No EndoH-sensitive TLN was detected in PS1$^{-/-}$ neurons, indicating a complete maturation. APP-CTF shows a dramatic accumulation (44-fold; mean ± SEM, $n = 3$).

of a potential intracellular domain of TLN can be measured via the activity of luciferase. Although for APP and Notch, nuclear translocation of the inducer fragment was prominent, and strongly inhibited by different γ-secretase inhibitors (125 nM DAPT, L685,458, or compound C), no signal could be detected with TLNΔE-Gal4VP16 (Fig. 2 B). To investigate whether the TLN transmembrane domain could be a γ-secretase substrate in the context of the APP protein, we swapped the transmembrane regions of TLN and APP to create an APP/TLN$_{TMR}$-chimaera. Even in this case no activity could be detected (Fig. 2 B). Therefore, we conclude that TLN is most likely not a γ-secretase substratum.

Finally, we investigated to what extent the TLN accumulations depended on γ-secretase activity. Treatment of wild-type neurons with γ-secretase inhibitors for 1 wk (daily administered from d 7–14) did not induce aberrant TLN accumulations (Fig. 2 C, left), although γ-secretase cleavage of APP-CTF was markedly inhibited (Fig. 2 C, right).

Of notice, in 25-d-old PS1$^{-/-}$ neurons the frequency of TLN accumulations did not further increase. Instead, in individual neurons they tended to be more numerous (grape-like) or larger (suggesting they may undergo fusion) (insets in Fig. 2 C). These accumulations were not encountered in PS1$^{+/-}$ neurons nor in neurons expressing human PS1 in a PS1$^{-/-}$ background (Qian et al., 1998). However, a true res-

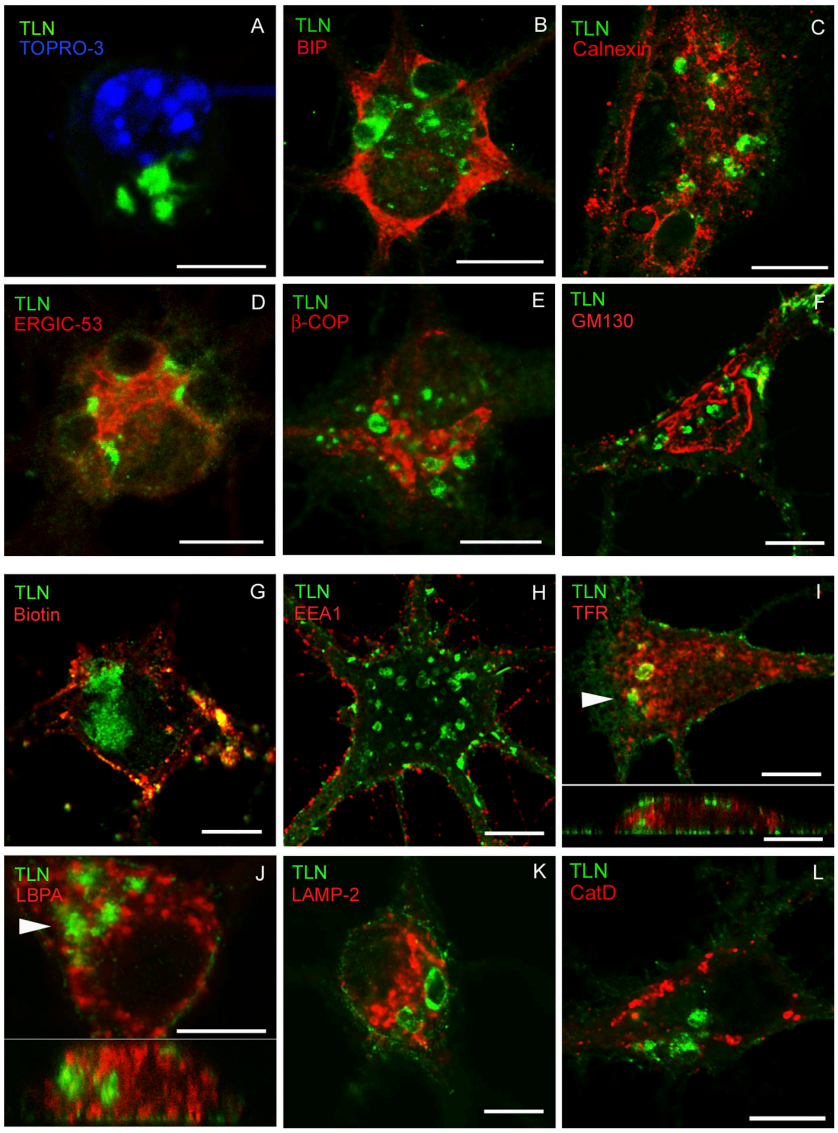

Figure 4. **TLN accumulation occurs in a compartment distinct from classic biosynthetic and endosomal pathways.** (A–F) Early compartments. No colocalization was observed between TLN (green in all panels) and nuclei (A, TOPRO-3), ER-markers BIP (B) and calnexin (C), ERGIC-53 (D), β-COP (E) or GM130 (F), and labeling cis-Golgi. (G–L) Late compartments. TLN accumulations are not accessible for exogenous biotin (G). Early and recycling endosomes (H, EEA1) and transferrin receptor (I, TFR), late endosomes (J, LBPA), and lysosomes (K, Lamp-2; L, catD) also stained negative for TLN. Vertical sections (x–z, arrowheads in I and J) clearly distinguish TLN accumulations from recycling (I, TFR) and late endosomes (J, LBPA). Bars, 10 μm.

cue was achieved by reintroducing human PS1 using adenoviral infection (Michiels et al., 2002). Increasing the multiplicity of infection (MOI) from 250 to 6,000 virus particles/neuron suppressed the frequency of TLN accumulations to wild-type levels (Fig. 2 D). Importantly, similar rescue effects were obtained with FAD-linked G384A or D257A dominant-negative PS1 mutants, arguing again for a γ-secretase–independent effect of PS1. Because TLN accumulations only appeared in ±30% of PS1$^{-/-}$ neurons, this full rescue could only be achieved with a very high transfection efficiency. Control adenoviral expression of eGFP indeed resulted in an 85–95% efficiency (unpublished data). Moreover, protein expression lasted up to 11 d after infection as shown for PS1 (Fig. 2 D). In summary, exogenous expression of wild-type or mutant PS1 is sufficient to restore the aberrant TLN phenotype.

The turnover of full-length TLN is affected in PS1$^{-/-}$ neurons

As PS1 is abundantly localized in pre-Golgi compartments (Annaert et al., 1999; Rechards et al., 2003), TLN accumulations may reflect a transport block in the early secretory pathway due to the absence of PS1. We tested this by analyzing the glycosylation kinetics of TLN. We overexpressed TLN using the SFV system in wild-type and PS1$^{-/-}$ cortical neurons and performed pulse-chase experiments in combination with endoglycosidase H (EndoH) treatment to quantify the ratio of mature to immature glycosylated TLN (Fig. 3 A). Phosphorimaging analysis revealed no statistical differences in this ratio, indicating that transport kinetics of newly synthesized TLN are similar in wild-type and PS1$^{-/-}$ neurons, as was seen for APP (Fig. 3 B; De Strooper et al., 1998).

However, using the same pulse-chase paradigm, we found that the half-life of newly synthesized TLN, but not full-length APP, was delayed in PS1$^{-/-}$ neurons (Fig. 3, A and B; bottom). If turnover is delayed, this should be reflected in a relative increase of endogenous TLN in PS1$^{-/-}$ neurons. Indeed, Western blotting and densitometric analysis showed an almost fourfold increase of TLN compared with wild-type neurons (Fig. 3 C). Interestingly, TLN appeared to be endoH resistant, suggesting that TLN accumulation occurs in post-Golgi compartments. Further controls indicated a weak accumulation of full-length APP and an impressive 44-fold increase in APP-CTF.

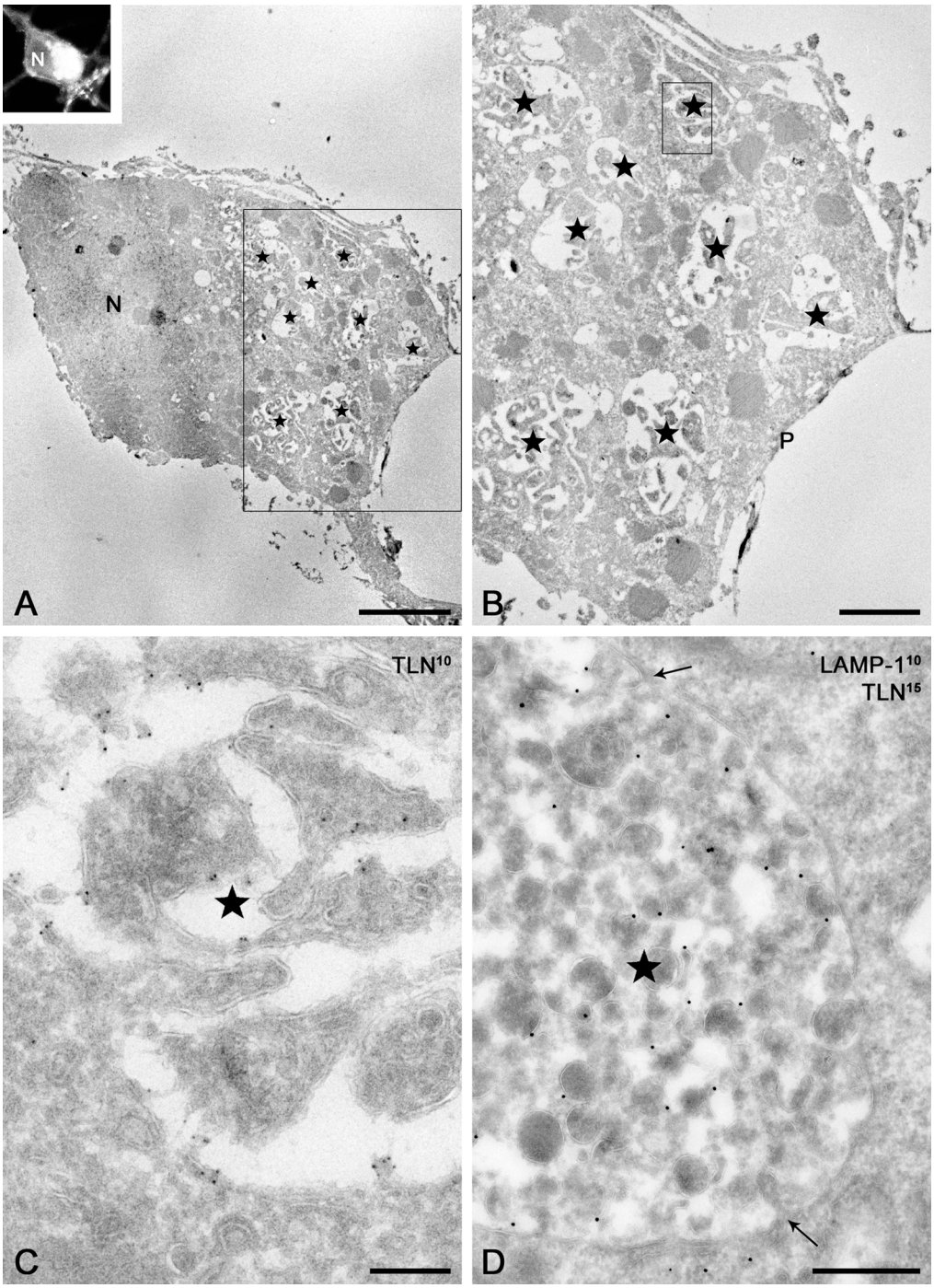

Figure 5. **Correlative light immuno-EM analysis of TLN accumulations.** (A) Insert: overview of the selected neuron as seen by immunocytochemistry. The bright signal for TLN reflects the numerous membranous accumulations seen at the ultrastructural immuno-EM level (star). (B) Higher magnification of the boxed area in A. (C) High magnification of the boxed structure seen in B. 10-nm gold particles label TLN. Note the complex composition of the internal membranes of the TLN-positive compartments. (D) Example of a TLN (15-nm gold)-containing structure obtained by the conventional cryosectioning technique. Note some heterogeneity in the internal membranes between C and D. Lamp-1 (10-nm gold) is absent from the TLN-containing compartment. Arrows point to invaginations of the cytoplasm. N, nucleus; P, plasma membrane. Bars: A, 5 μm; B, 2 μm; C, 500 nm; D, 200 nm.

TLN accumulations do not codistribute with "classical" early and late compartments

To understand the possible mechanism(s) behind the increased protein levels and delayed turnover, we set out to identify the compartment where TLN accumulates in PS1$^{-/-}$ neurons. First, TLN accumulations could not be identified as nuclear inclusions (Fig. 4 A), and essentially no overlap was detected with marker proteins of the ER such as BIP and calnexin (Fig. 4, B and C). Other compartments of the early secretory pathway, including the intermediate compartment (ERGIC-53) and Golgi apparatus (β-COP and GM130), were equally devoid of TLN immunostaining (Fig. 4, D–F).

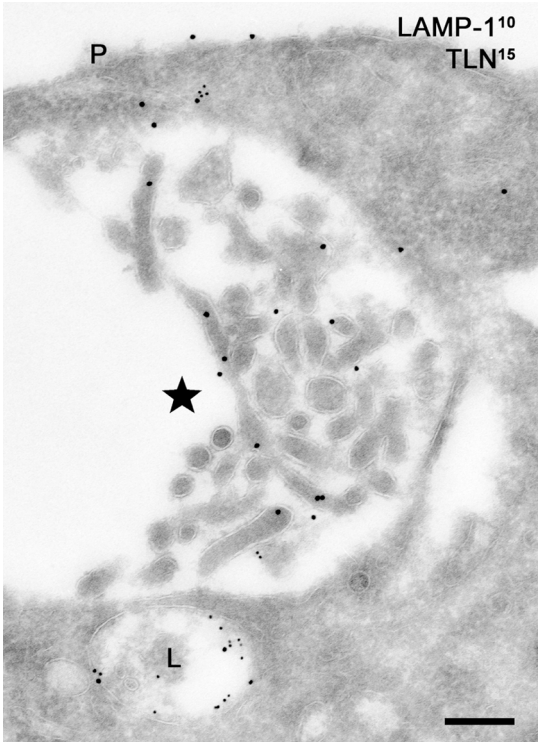

Figure 6. **TLN accumulations are distinct from lysosomes.** A TLN (15-nm gold)-containing structure as obtained by the conventional cryosectioning technique double labeled with Lamp-1 (10-nm gold). The TLN-positive compartment is clearly distinct in size and from lysosomes (L) and lacks Lamp-1. P, plasma membrane. Bar, 200 nm.

Although TLN accumulations are found close beneath the cell surface (Annaert et al., 2001), they were not accessible to exogenous biotin (Fig. 4 G). We detected no association with early (EEA1) or recycling endosomes (transferrin receptor) (Fig. 4, H and I), nor with late endosomes (LBPA) and lysosomes (Lamp-2 and cathepsin D [catD]).

These findings encouraged us to implement EM. Due to the specifications of the culture, we applied a new flat-embedding technique that preserves the in situ orientation of polarized neurons (Oorschot et al., 2002), and combined this with correlative light immuno-EM (Koster and Klumperman, 2003). This allowed us to localize TLN accumulations before EM processing (Fig. 5, inset). Immuno-EM revealed abundant gold label at the plasmalemma and in large membrane-bound vacuoles. In these structures, label was found both on the limiting membrane and internal membranes. Interestingly, LAMP-1 labeled lysosomes, but not TLN positive structures (Fig. 6), confirming that they are distinct from (pre)lysosomal compartments. Except for their large size, their heterogeneous content including tubular and vesicular structures is suggestive for an autophagic origin.

Characterization of TLN-positive autophagic vacuole-like structures

Autophagy is the intracellular bulk degradation system and plays an important role in the cellular protein economy (Mizushima et al., 2002). To further identify TLN-positive structures, we first analyzed the uptake of monodansylcadaverine (MDC), a compound used to identify autophagic vacuoles (Munafo and Colombo, 2001). MDC coaccumulated with TLN in PS1$^{-/-}$ neurons (Fig. 7 A). Noteworthy, MDC uptake occurred in the absence of starvation, indicating that TLN accumulations are preexisting structures.

Autophagic vacuoles originate from an elongation process of isolation membranes that close and finally fuse with late endosomes/lysosomes (Mizushima et al., 2002). Several ubiquitin-like conjugation systems are essential for autophagic vacuole formation. Among them, the Apg12p–Apg5p conjugate is important in the initial steps where it localizes (albeit a small fraction) to the outer side of the isolation membrane throughout the elongation process, and dissociates again upon completion of the autophagic vacuole (Mizushima et al., 2001). A second protein is LC3 (Kabeya et al., 2000), which remains partially on the autophagic vacuole even after fusion with lysosomes. In PS1$^{-/-}$ neurons, both anti-Apg12p and -LC3 antibodies immunostained TLN accumulations (Fig. 7, B and C). However, Apg12p remains stably associated with these structures, which is surprising because this protein is reported to dissociate before or upon closure of the autophagic vacuole. This suggests that the normal formation and maturation of this type of autophagic vacuole is impaired in PS1$^{-/-}$ neurons. In wild-type neurons, no colocalization of Apg12p and LC3 with TLN was observed (Fig. 7, B and C, top row), demonstrating the unique nature of the accumulations. Interestingly, in some PS1$^{-/-}$ neurons small TLN- and Apg12p-positive structures were detected in the proximal regions of dendrites, possibly representing earlier stages of accumulation (Fig. 7 B, bottom row).

TLN localizes to autophagic vacuoles in catD$^{-/-}$ hippocampal neurons

These surprising findings prompted us to investigate in more detail the relationship of TLN with autophagic vacuoles. In many cases, autophagic vacuole accumulation is associated with defective lysosomal biogenesis (Koike et al., 2000; Eskelinen et al., 2002). However, in our case no difference in catD maturation was found between wild-type and PS1$^{-/-}$ neurons, and lysosomal delivery of catD is therefore not impaired (Fig. 8 A). On the other hand, catD deficiency results in the accumulation of autophagic vacuoles/autophagosomes (Koike et al., 2000). This is also true in primary hippocampal neurons derived from catD$^{-/-}$ embryos, as can be observed with Lysotracker (Fig. 8 B). Although TLN accumulations are clearly not acidified in PS1$^{-/-}$ neurons (Fig. 8 C), acidic organelles were often found in close apposition and likely represent lysosomes (Fig. 6). Surprisingly, in catD$^{-/-}$ neurons some TLN immunoreactivity was detected in the large Lysotracker-positive organelles (Fig. 8 C, bottom). Ultrastructurally, these TLN-positive organelles resemble dense autophagic vacuole-like structures (Fig. 8 D). Importantly, these organelles are smaller in diameter compared with TLN accumulations and were not seen in wild-type or PS1$^{-/-}$ neurons. Together, in catD$^{-/-}$ neurons TLN localizes to autophagic vacuoles, suggesting that these organelles are part of the normal physiological route for TLN degradation.

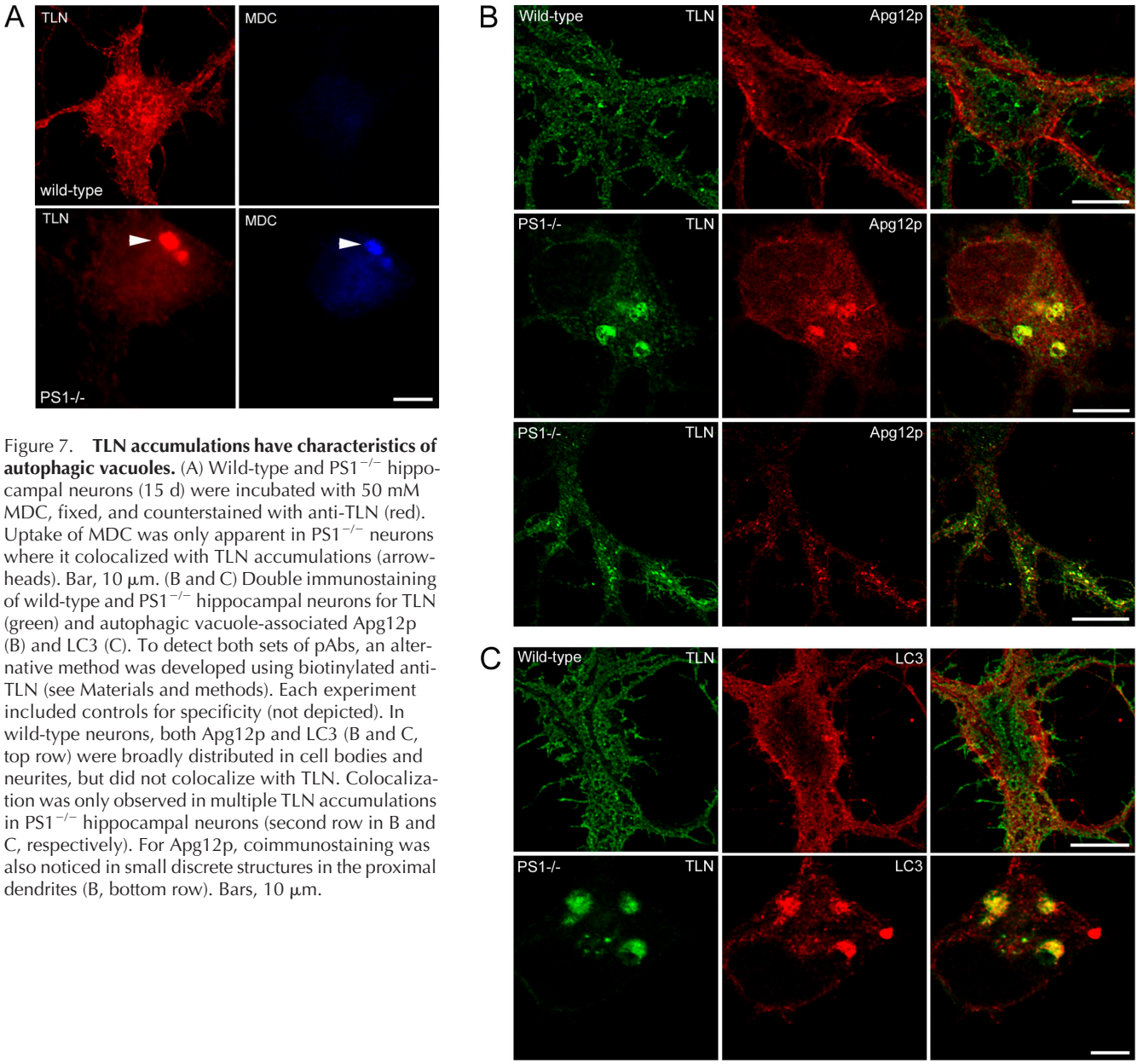

Figure 7. **TLN accumulations have characteristics of autophagic vacuoles.** (A) Wild-type and PS1$^{-/-}$ hippocampal neurons (15 d) were incubated with 50 mM MDC, fixed, and counterstained with anti-TLN (red). Uptake of MDC was only apparent in PS1$^{-/-}$ neurons where it colocalized with TLN accumulations (arrowheads). Bar, 10 μm. (B and C) Double immunostaining of wild-type and PS1$^{-/-}$ hippocampal neurons for TLN (green) and autophagic vacuole-associated Apg12p (B) and LC3 (C). To detect both sets of pAbs, an alternative method was developed using biotinylated anti-TLN (see Materials and methods). Each experiment included controls for specificity (not depicted). In wild-type neurons, both Apg12p and LC3 (B and C, top row) were broadly distributed in cell bodies and neurites, but did not colocalize with TLN. Colocalization was only observed in multiple TLN accumulations in PS1$^{-/-}$ hippocampal neurons (second row in B and C, respectively). For Apg12p, coimmunostaining was also noticed in small discrete structures in the proximal dendrites (B, bottom row). Bars, 10 μm.

TLN mediates phagocytic uptake of microbeads in primary hippocampal neurons

We have shown that TLN accumulations do not share endosomal/lysosomal components. Also, TLN normally localizes to the somatodendritic plasma membrane and accumulates as a mature protein (Fig. 3 C), suggesting that accumulations originate from the plasma membrane through an internalization event distinct from endocytosis. To test whether phagocytosis is involved, we triggered this process by challenging hippocampal neurons with 2-μm microbeads. After 4 h, many beads were already found associated with neurites, and recruited TLN immunoreactivity (Fig. 9 A, top). Longer incubations (24 or 48 h; Fig. 9 A, bottom) resulted in a complete redistribution of TLN to microbeads. Because actin polymerization is considered the driving force of phagosome cup formation (May and Machesky, 2001), we costained with phalloidin-Alexa 568. Actin polymerization clearly colocalizes in a ring- or cup-shaped pattern with TLN on individual microbeads (Fig. 9 B; Video 1, available at http://www.jcb.org/cgi/content/full/jcb.200406060/DC1). Although the exact mechanism in phagosome formation is not clear, regulation by local phosphoinositide production is crucial in actin polymerization. Indeed, and next to actin, also endogenous phosphatidylinositol 4,5 bisphosphate (PIP2) is recruited to the TLN-positive phagosomal cup (Fig. 9 C, arrowheads in boxed area). Interestingly, PIP2 also colocalized to discrete TLN spots probably representing normal plasma membrane localization of TLN (Fig. 9 C, asterisk). Notably, levels of PIP2 between different TLN-positive microbeads were sometimes very variable. This may reflect different stages of phagosome formation because PIP2 is rapidly lost upon phagosome sealing and completion due to the recruitment of PLC (Botelho et al., 2000). In agreement

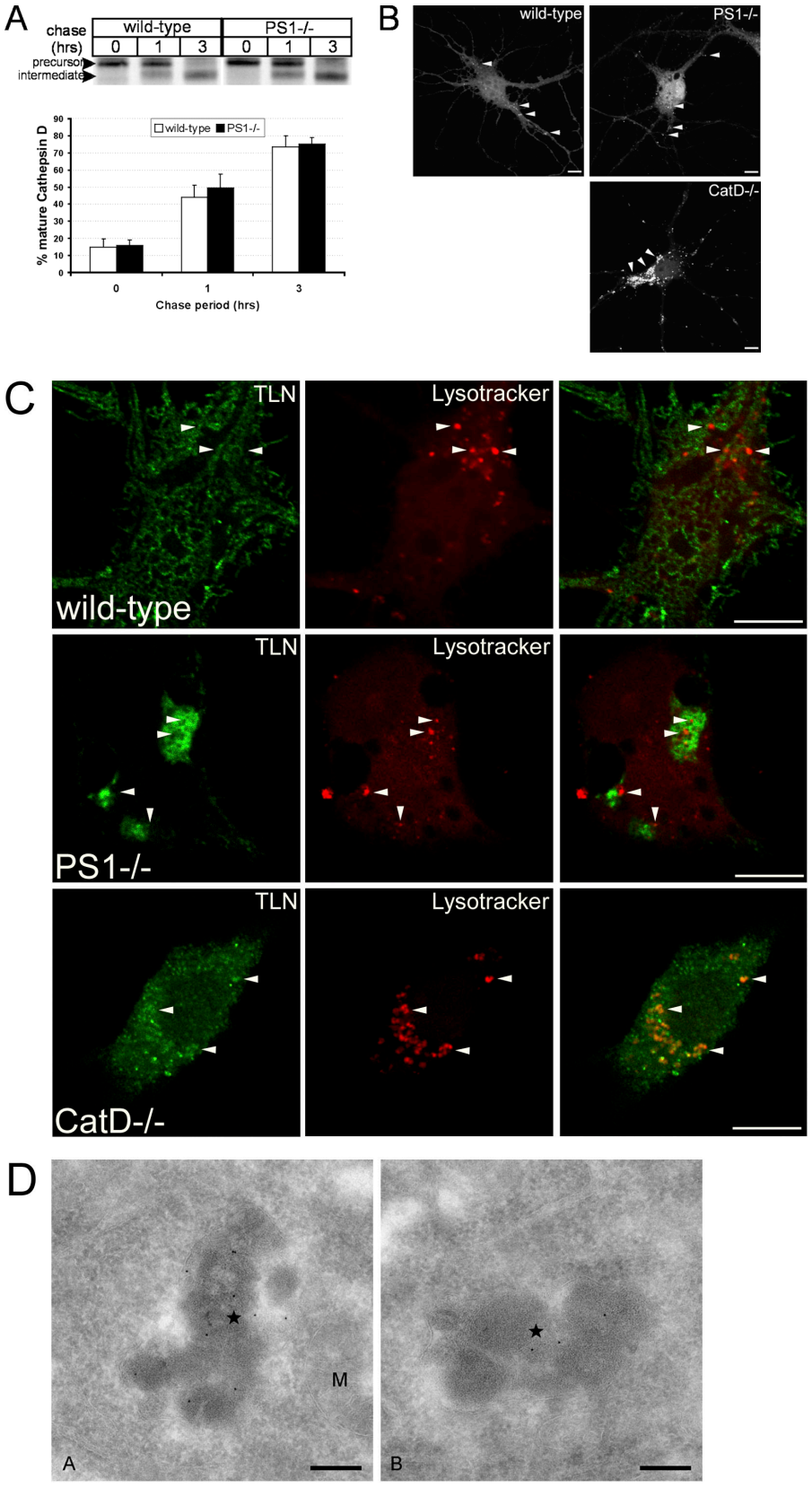

Figure 8. **CatD$^{-/-}$ hippocampal neurons as a model system for autophagic vacuole accumulation.** (A) Intracellular sorting and maturation of catD. Wild-type and PS1$^{-/-}$ neurons were metabolically labeled and chased for the indicated time periods. Phosphorimaging of immunoprecipitated radiolabeled catD did not reveal a difference in the ratio of proteolytically processed 46-kD intermediate vs. 52-kD precursor (mean ± SEM, $n = 3$). (B–D) TLN localizes to autophagic vacuoles of catD $^{-/-}$ hippocampal neurons. Lysotracker staining revealed sparsely distributed small-sized organelles in wild-type and PS1$^{-/-}$ neurons in contrast to catD$^{-/-}$ neurons where high numbers of large Lysotracker-positive organelles were found (B, arrowheads). Although TLN accumulations in PS1$^{-/-}$ were fully negative for Lysotracker, some acidic organelles tended to closely associate (C, arrowheads, middle). In catD$^{-/-}$ neurons, TLN was clearly detected in the large acidic organelles (C, bottom). Bars, 20 μm. (D) At the immuno-EM level, the large acidic organelles seen in catD$^{-/-}$ neurons represent dense autophagic vacuole-like structures (star) that label positive for TLN (10-nm gold). M, mitochondrion. Bars, 200 nm.

with this, no (or almost no) PIP2 was detected on TLN accumulations in PS1$^{-/-}$ neurons. Microbead uptake was equally observed both in wild-type and PS1$^{-/-}$ neurons, indicating that this phagocytic process most likely does not require PS1. Nevertheless, our data may provide a first insight in the initial steps of the subcellular route that leads to the aberrant TLN phenotype in PS1$^{-/-}$ hippocampal neurons.

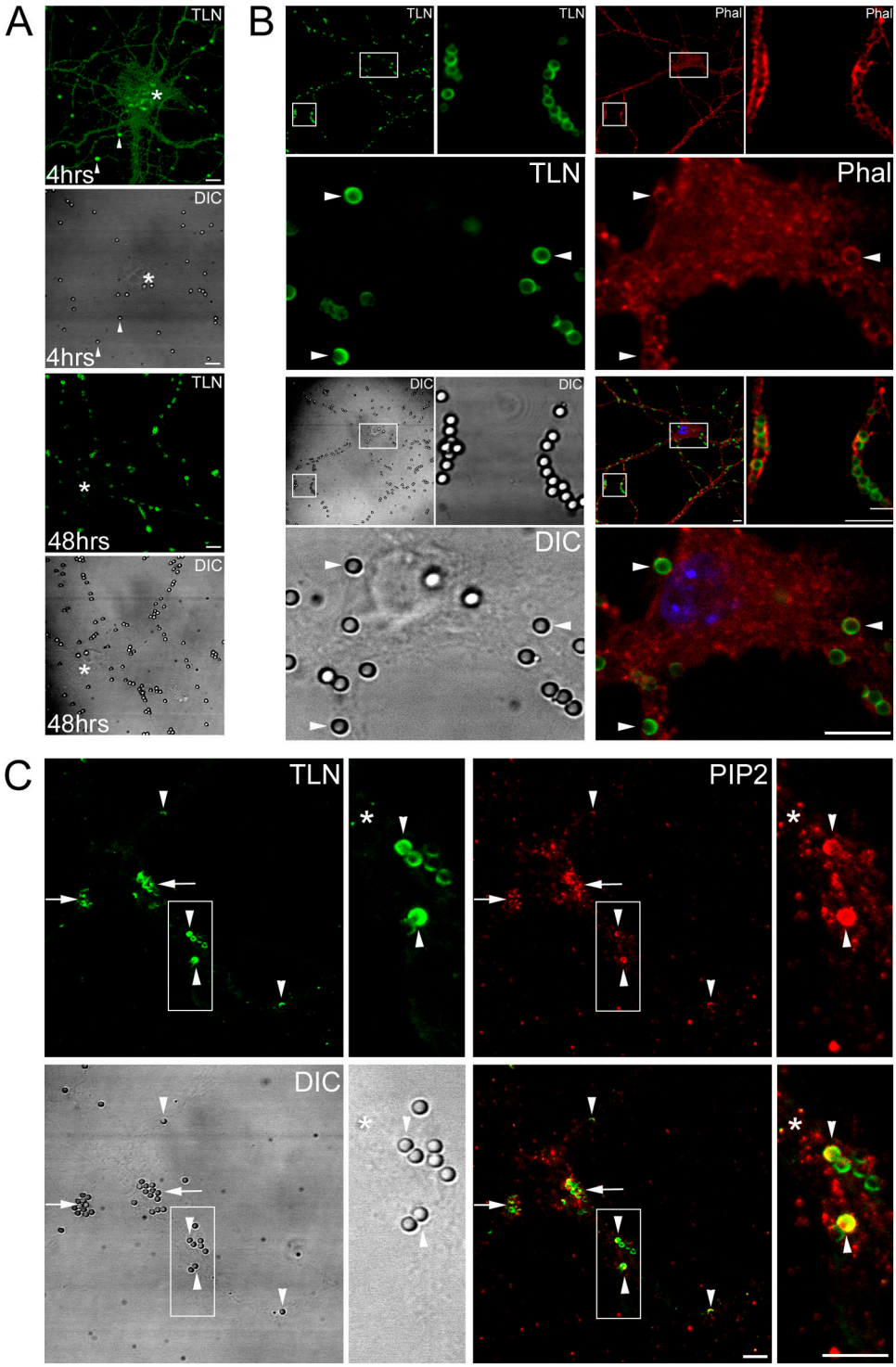

Figure 9. **TLN mediates phagocytic uptake of microbeads in hippocampal neurons.** (A) Microbeads align along neurites of hippocampal neurons as demonstrated by phase contrast (DIC). Already after 4 h, many beads stain positive for TLN (arrowheads, top). At 48 h (bottom), most TLN immunoreactivity was associated with microbeads at the expense of its typical plasma membrane staining. *, cell body. Note that microbeads were not found associated with preexisting TLN accumulations (asterisk in top panels, 4 h). (B) Microbeads (24 h) accumulate TLN and actin, as shown by phalloidin-Alexa 568. An overview of the neuron is given in each top left inset, next to two detailed areas (white boxes). The differential interference contrast (DIC) clearly demonstrates a complete colocalization of microbeads with TLN and phalloidin (arrowheads). TOPRO-3 (blue) marks the nucleus (see also Fig. S1, available at http://www.jcb.org/cgi/content/full/jcb.200406060/DC1). (C) Similar as in B, but immunostained for TLN and endogenous PIP2. The overview demonstrates the overall recruitment of PIP2 to microbeads (arrows). The parallel insets show a detailed area (white box) with PIP2 being colocalized with TLN on individual microbeads (arrowheads). Note that PIP2 occasionally colocalizes with TLN at the plasma membrane (asterisk). Bars (A–C), 10 μm.

Discussion

We previously documented the specific interaction of APP and TLN with PS1 in neurons (Annaert et al., 2001), while leaving open two major issues concerning γ-secretase processing and missorting of TLN in PS1$^{-/-}$ neurons. Here, we demonstrate convincingly that TLN is not a γ-secretase substrate (which is surprising given the growing list of type I integral membrane proteins that are cleaved by this activity), and identify important steps in the transport route that ultimately result in TLN accumulations. First, we never detected TLN-CTF accumulating in PS1$^{-/-}$ cells, a feature reminiscent of all reported substrates. Second, using a sensitive Gal4-VP16–based reporter assay (Struhl and Adachi, 2000), we observed no transcriptional activation resulting from the release of the cytoplasmic domain of TLNΔE or when the TMR of TLN was swapped into APP. Pulse-chase experiments demonstrated furthermore an increased half-life of TLN and an almost fourfold increase of TLN protein expression levels in PS1$^{-/-}$ neurons. These and previous data (Annaert et al., 2001) clearly suggest that full-length TLN is delayed in turnover. This coincides with the accumulation of TLN in distinct organelles in PS1$^{-/-}$ hippocampal neurons that have features of autophagic vacuoles as they could be immunolabeled for Apg12p and LC3.

Our findings that TLN is not a γ-secretase substrate contradict the hypothesis of Struhl and Adachi (Struhl and Adachi, 2000), who assayed the substrate requirements for γ-secretase cleavage and proposed that although the particular sequence of the transmembrane domain is of less importance, any type I membrane protein can become a substrate once the ectodomain is sufficiently shortened. To date, TLN is now the first type I transmembrane protein described that does not obey this rule.

Because the confocal microscopy approach did not disclose the nature of the TLN accumulations, we extended the analysis to the ultrastructural level and combined a novel embedding technique (Oorschot et al., 2002) with correlative light immuno-EM. This work revealed autophagic characteristics for the TLN accumulations, which was confirmed next by labeling with MDC and coimmunostaining for Apg12p and LC3. Both proteins are members of ubiquitin-like conjugation systems that sequentially associate and regulate the formation of autophagic vacuoles (Mizushima et al., 2002). Furthermore, the absence of late endosomal and lysosomal marker proteins as well as Lysotracker indicated that the TLN-positive vacuoles did not yet fuse with the endosomal/lysosomal system and were not acidified. Interestingly, acidification of autophagic vacuoles is essential for the fusion with lysosomes (Yamamoto et al., 1998). Although this suggests that TLN accumulations resemble initial autophagic vacuoles, several important differences were noticed. First, their size is exceptionally large (exceeding 2 μm) compared with intermediate autophagic vacuoles (between 400 and 800 nm) (Fig. 5, Fig. 8 D, compare with autophagic vacuoles in catD$^{-/-}$ neurons; Eskelinen, 2004). Second, we never encountered ribosomes, ER membranes, or mitochondria in these structures, although they represent the major contents of true autophagic vacuoles. Third, at the ultrastructural level we never observed a double-limiting membrane. Still, this should be present if TLN accumulations would originate from an elongating isolation membrane. Because the major criteria are not met, the TLN accumulations cannot be classified as classic autophagic vacuoles, and hence their origin may be uniquely different.

Because intense gold labeling for TLN was recovered on all internal membranes and because TLN has a plasma membrane localization, we argued that the TLN accumulations directly originated from the plasma membrane through phagocytosis or macropinocytosis. Phagocytosis is an internalization route abundantly used by certain cell types such as macrophages to take up large particles. As far as we know, phagocytosis has not been studied in hippocampal neurons, and receptors that trigger this event are not identified. However, administration of 2-μm microbeads (a widely accepted method to assay phagocytosis) to hippocampal neurons in culture resulted over time in a redistribution and clustering of endogenous TLN toward phagosome cups. Because we did not observe microbead uptake in HeLa cells or inhibitory neurons that do not express TLN, these data strongly suggest that TLN may be a candidate receptor triggering phagocytosis, as similarly described for the Fc receptor in macrophages (Greenberg and Grinstein, 2002). Interestingly, two other characteristics of phagosome initiation, actin polymerization and PIP2 recruitment, were equally detected on TLN-positive phagosome cups, suggesting that identical signaling cascades are involved.

The brain area–specific expression of TLN (Yoshihara et al., 1994) indicates that the TLN-mediated route for degradation is unique to a limited number of neurons including hippocampal neurons. In this respect, it is interesting to mention that Lee and coworkers (Wilson et al., 2004) also demonstrated an accumulation of degradative organelles in PS1$^{-/-}$ mixed cortical neurons, but in contrast to hippocampal neurons, these were Lamp-2– and catD-positive. Also, their diameter is much smaller and morphologically they resemble late autophagic vacuoles reminiscent of those observed in catD$^{-/-}$ (this paper) or Lamp-2$^{-/-}$ cells (Eskelinen et al., 2002). Similar accumulations of degradative organelles are seen in PS1/2-deficient fibroblasts (Wilson et al., 2004), and again in contrast to hippocampal neurons they could be stained with Lysotracker (unpublished data), indicating that they fused with (late) endosomes. Finally, and opposed to Wilson et al. (2004), we did not observe α-synuclein in the TLN accumulations (Video 2, available at http://www.jcb.org/cgi/content/full/jcb.200406060/DC1), further underscoring their unique origin. Because the formation of TLN-positive phagosome cups triggered by microbeads was virtually identical in wild-type and PS1$^{-/-}$ hippocampal neurons (unpublished data), our data collectively favor the idea that PS1 deficiency affects not the initial, but final stages of protein degradation at a step before fusion with prelysosomes or lysosomes. This results in the accumulation of classic late autophagic vacuoles in PS-deficient mouse embryonic fibroblasts or PS1$^{-/-}$ cortical neurons (Wilson et al., 2004), or TLN-positive autophagic vacuole-like structures originating from phagocytic organelles specifically in the case of hippocampal neurons (this paper).

How PS1 interferes at the molecular level remains to be investigated in more detail, but data point out already that impaired γ-secretase processing of a yet unknown substrate

involved in autophagic vacuole maturation is unlikely to be responsible for this phenomenon because TLN accumulations could not be induced by γ-secretase inhibitors and the TLN phenotype could be rescued by adenoviral expression of the dominant-negative D257A PS1 mutant. From a medical point of view, this implies that compounds that block γ-secretase activity will not block this function of PS1.

We consistently detected both Apg12p and LC3 on TLN accumulations, suggesting that the maturation of the TLN-positive degradative organelle is not accompanied by the dissociation of the Apg12p–Apg5p conjugate, as would be expected in normal autophagy. Therefore, PS1 may be required in the sequence of proper dissociation of the Apg12p–Apg5p conjugate or in the targeting of LC3 to the limiting membrane. LC3 exists in two molecular forms, LC3-I and LC3-II, of which only the latter is specifically bound to the autophagic vacuole (Kabeya et al., 2000). Interestingly, in PS1/2-deficient mouse embryonic fibroblasts, starvation-induced autophagy resulted in only a low modification rate of LC3-I to its membrane-associated LC3-II form (Fig. S1, available at http://www.jcb.org/cgi/content/full/jcb.200406060/DC1).

Alternatively, our observations may link PS1 to a role in trafficking as suggested by several papers. For instance, the cell surface accumulation of APP in $PS1^{-/-}$ is explained by a delayed internalization rate of APP (Kaether et al., 2002) or a retention function for PS1 in the early secretory pathway (Cai et al., 2003). On the contrary, nicastrin fails to become mature glycosylated in PS-deficient cells, pointing to a chaperone function for PS1 in early compartments. Although none of these papers resemble or explain the observed blockade in TLN turnover at late stages, they correlate with the different subcellular pools of PS1. Indeed, in neurons PS1 is abundantly distributed in the soma and dendrites and localizes predominantly to the ER and intermediate compartment (Annaert et al., 1999). Because we have demonstrated that this major pool is not associated with γ-secretase activity (Cupers et al., 2001; Maltese et al., 2001), its abundancy in the intermediate compartment and COPI-coated organelles (Rechards et al., 2003) supports a regulatory transport function at this step in the secretory pathway. In addition, small but significant pools were observed at the cell surface and endosomes/lysosomes (Kaether et al., 2002; Pasternak et al., 2003; Rechards et al., 2003). Although these pools may represent the γ-secretase active pools, they may also contribute to APP internalization and lysosome fusion, respectively.

Accumulation of autophagic vacuoles is observed in an increasing number of neurodegenerative diseases including Alzheimer's, Huntington's, and Parkinson's disease, and various prion diseases (for review see Larsen and Sulzer, 2002). In the case of sporadic Alzheimer's disease, mainly an activation of the endocytic pathway and increased delivery of lysosomal enzymes to endosomes has been observed in neurons (Cataldo et al., 1997; Mathews et al., 2002). In most other cases, a salient feature of autophagic vacuole accumulation is the presence of lysosomal enzymes such as CatD (Kegel et al., 2000). In addition, impaired capacity for lysosomal degradation and mistargeting of lysosomal enzymes is clearly the main reason for autophagic vacuole accumulation in lamp-2 and catD knockouts (Tanaka et al., 2000; Eskelinen et al., 2002). In the latter model, endogenous TLN also localized to accumulating autophagic vacuoles, arguing that this is indeed the physiological route for TLN turnover in the wild-type neuron. The accumulation of TLN-positive structures in $PS1^{-/-}$ neurons is different, as it was not accompanied with lysosomal fusion or impaired catD maturation. Also, their origin is likely not the classical autophagic pathway initiated by the formation of an isolation membrane, but maybe by a direct recruitment of autophagic vacuole protein complexes to the limiting membrane of phagocytic organelles after fission from the plasma membrane. How these protein complexes are recruited is currently unknown and requires further investigation.

In this paper we provide evidence that the TLN interaction links PS1 to a new modulatory role in the maturation and fusion of late autophagic vacuoles with lysosomes at the final step of autophagy. This extends the role of PS1 in protein turnover to at least three independent pathways: intramembrane proteolysis through its γ-secretase catalytic activity, the cytosolic loop domain–associated β-catenin turnover, and now autophagic vacuole degradation. It will now become important to define the precise molecular mechanism and the domains in this multifaceted protein that are critically involved. Because autophagic vacuole accumulation is observed in several neurodegenerative diseases, elucidating the role of PS1 in autophagic vacuole maturation and specifically in their fusion with lysosomes has therefore not only repercussions for our further understanding of the cell biology of this protein, but is also anticipated to contribute to the further understanding of these pathologies.

Materials and methods

Materials and antibodies

Cell culture media were from GIBCO BRL. TOPRO-3 and phalloidin-Alexa 568 (Molecular Probes, Inc.) were used to label nuclei and actin. MDC was from Sigma-Aldrich. γ-Secretase inhibitors were from Calbiochem (X or L685,458), Elan (DAPT), and AstraZeneca (Compound C).

Polyclonal anti-PS1-NTF (B19.2), -CTF (B32.1) and -TLN (B36.1) have been described previously (Annaert et al., 2001). B63.1 and B59.1 were generated using a synthetic peptide mimicking the final 16 and 18 amino acids of APP and nicastrin, respectively, coupled to KLH (Pierce Chemical Co.). Mab 9C3 against nicastrin was produced by immunizing the same peptide in balb/c mice followed by generation of a hybridoma cell line according to established procedures. We acknowledge the antibody gifts of anti-calnexin (A. Helenius, ETH Zurich, Zurich, Switzerland), anti-ergic-53 (J. Saraste, University of Bergen, Bergen, Norway) -LC3 (T. Yoshimori, National Institute of Genetics, Shizuoka-ken, Japan), -Apg12 (N. Mizushima, National Institute for Basic Biology, Okazaki, Japan), PIP2 (G. Hammond, Cancer Research Institute, London, UK), -LBPA (J. Gruenberg, University of Geneva, Geneva, Switzerland), and -APP COOH terminus (c 1/6.1; P. Mathews, Nathan Kline Institute, Orangeburg, NY). Mabs to Lamp-2 (Abl-93) were obtained from Developmental Studies Hybridoma Bank (Iowa City, Iowa); anti-synaptophysin (cl.7.2) and anti-PS1-CTF (mAb 5.2) were from R. Jahn (MPI-Göttingen, Göttingen, Germany) and B. Cordell (Scios Inc., Sunnyvale, CA). mAbs to GM130 and EEA1 were from BD Biosciences, the transferrin receptor from Zymed Laboratories, β-COP from Sigma-Aldrich, and BIP from StressGen Biotechnologies.

Constructs and γ-secretase luciferase assay

pSFV constructs encoding human APP, murine TLN, and TLNΔE have been described previously (Annaert et al., 2001). APP and NotchΔE were cloned into the EcoRV site in front of the Gal4VP16 sequence in pIP-AdApt vector. A construct encoding 10 aa of the ectodomain, the transmembrane and cytosolic domains of TLN was obtained by PCR and ligated in pGEMT containing the TLN signal peptide (SP). SP-TLNΔE was

next cloned into pIPAdApt and GAL 4VP16 was inserted, resulting in a pIPAdApt-SP-TLNΔE-Gal4-VP16 construct. For the APP/TLN_{TMR} chimaera, the coding region for APP-TMR was replaced by a PCR fragment encoding the TLN-TMR.

Luciferase assay

Hela cells were transfected with 200 ng pFRluc plasmid (UAS-responsive luciferase construct; Stratagene) and 200 ng inducer plasmid using FuGENE (Roche). After 24 h, cells were incubated with or without inhibitors (125 nM), and after 16 h were lysed and assayed (Victor2; PerkinElmer).

Primary neuron cultures and metabolic labeling

Human PS1 (in a $PS1^{-/-}$ background [Qian et al., 1998]), wild-type, $PS1^{+/-}$, $PS1^{-/-}$, or $catD^{-/-}$ primary hippocampal neurons were derived from E17 embryos out of heterozygous crosses and were cocultured with a glial feeder layer (Goslin and Banker, 1991; Annaert et al., 1999). For metabolic pulse-chase labeling, mixed cortical neuron cultures from wild-type and $PS1^{-/-}$ were prepared (Annaert et al., 1999; De Strooper et al., 1998).

At the end, neurons were extracted and immunoprecipitated fractions were treated with 10 mU endopeptidase H (Boehringer) before SDS-PAGE (NuPAGE; Invitrogen) and phosphorimaging (Typhoon; PerkinElmer).

For Western blotting, 10–12-d-old hippocampal cultures were harvested in PBS, pelleted, resuspended in sample buffer, and separated on SDS-PAGE. Blots were detected using chemiluminescence (WesternLite; PerkinElmer) and were scanned using an internal standard (ImageScanner and TotalLab; Amersham Biosciences).

Adenoviral infection

cDNAs of human wild-type, familial Alzheimer's disease–linked G384A, or a dominant-negative D257A mutant PS1 were constructed into the pIPspADApt6 adaptor plasmid, which contains part of the adenoviral genome. cDNA encoding eGFP was used as a control. Adenoviruses were generated by cotransfection with helper cosmid DNA in the PER.C6/E2A adenoviral packaging cells and titers were determined (Michiels et al., 2002). For rescue experiments, $PS1^{-/-}$ hippocampal neurons grown for 4–6 d on coverslips (at a density of 800–1,200 neurons/coverslip) were infected overnight with different viruses at different MOIs (250–6,000) and were returned to conditioned medium until fixation on d 15.

Confocal laser scanning microscopy

Primary hippocampal neurons (14–25 d) were fixed in 4% PFA/4% sucrose in 0.1 M phosphate buffer (30 min, RT), permeabilized by methanol/acetone (−20°C), 0.5% Triton X-100/PBS, or 0.5% saponin (5 min), and processed for indirect immunofluorescence (Annaert et al., 2001). Alexa 488– and 568–conjugated secondary antibody (Molecular Probes, Inc.) stainings were detected through a Diaphot 300 (Nikon) connected to a confocal microscope (MRC 1024; Bio-Rad Laboratories). Data were collected using Lasersharp 3.0 and processed in Adobe Photoshop 7.0.

For double immunocytochemistry using pAbs of the same host species, blocked and permeabilized neurons were incubated overnight with biotinylated anti-TLN (B36.1). After blocking free sites with unconjugated Fab fragments (goat anti–rabbit; Jackson ImmunoResearch Laboratories), coverslips were incubated (for 1 h) with Alexa 488–conjugated streptavidin (Molecular Probes, Inc.) followed by second primary antibody and Alexa 568–conjugated goat anti–rabbit. In some cases neurons were incubated with biotin (Pierce Chemical Co.), Lysotracker (Molecular Probes, Inc.), or 50 mM MDC for 30 min at 4 or 37°C before fixation and counterstaining with anti-TLN. For MDC, analysis was done on a microscope (DMRB; Leica) equipped with a UV detection filter set (excitation wavelength 380 nm, emission filter 525 nm), a CCD camera (Photometrics Ltd.), and QuipsFISH software (Vysis). To study phagocytic uptake, 14-d-old neurons were incubated (4–48 h) with 2-μm microbeads (50/cell; Polysciences) in conditioned medium, briefly washed, fixed, and processed for immunocytochemistry.

Immuno-EM

Fixed neurons were quenched (50 mM NH_4Cl, 5 min) and briefly permeabilized in 0.2% Triton X-100, followed by incubation with B36.1. After washing, cells were incubated with Alexa 488–conjugated goat anti–rabbit IgG to identify TLN accumulations. Positively identified neurons were further processed for immuno-EM using a flat embedding technique (Oorschot et al., 2002; Koster and Klumperman, 2003). The resulting ultrathin cryosections were labeled with anti-Alexa 488 IgG (Molecular Probes, Inc.) according to the protein A–gold technique. Alternatively, cells were labeled with B36.1 and anti-Lamp-1, scraped and incubated with protein A–gold (Slot et al., 1991).

Miscellaneous

Microsomal fractions of cortices of E17 wild-type and $catD^{+/-}$ and $catD^{-/-}$ embryos were either analyzed by Western blotting or assayed for γ-secretase activity using a cell-free assay. In brief, 2% CHAPS extracts were incubated overnight with recombinant APP-C99, and newly produced amyloid β was detected by Western blotting (Nyabi et al., 2003).

Online supplemental material

Video 1 shows three-dimensional (3D) reconstructions of the neuronal cell body displayed in Fig. 9 B for phalloidin-Alexa 568, TLN (green, Alexa 488 goat anti–rabbit), and the merged 3D. Video 2 shows 3D reconstructions of a neuronal cell body double immunostained for α-synuclein (Alexa 568 goat anti–mouse) and TLN (Alexa 488 goat anti–rabbit), as well as the merged file. Fig. S1 shows a Western blot analysis for LC3 processing in wild-type, PS1/2 knockout mouse embryonic fibroblasts, and PS1/2 knockout fibroblasts rescued with PS1 wild-type or dominant-negative aspartate mutants. Online supplemental material available at http://www.jcb.org/cgi/content/full/jcb.200406060/DC1.

The authors wish to thank Marlies Rusch for $catD^{-/-}$ mice and Eeva-Liisa Eskelinen for stimulating discussions. Dirk Adriaensen is acknowledged for improvement of the immunocytochemistry.

This work was financed by the Flanders Interuniversity Institute for Biotechnology (VIB), and by grants of the FWO-Vlaanderen (G.0377.02), KULeuven (GOA/2004/12), IARF-Belgium/Netherlands (to W. Annaert and J. Klumperman), and IWT (to C. Esselens).

Submitted: 10 June 2004
Accepted: 9 August 2004

References

Annaert, W., and B. De Strooper. 2002. A cell biological perspective on Alzheimer's disease. *Annu. Rev. Cell Dev. Biol.* 18:25–51.

Annaert, W.G., L. Levesque, K. Craessaerts, I. Dierinck, G. Snellings, D. Westaway, P.S. George-Hyslop, B. Cordell, P. Fraser, and B. De Strooper. 1999. Presenilin 1 controls γ-secretase processing of the amyloid precursor protein in pre-Golgi compartments of hippocampal neurons. *J. Cell Biol.* 147:277–294.

Annaert, W.G., C. Esselens, V. Baert, C. Boeve, G. Snellings, P. Cupers, K. Craessaerts, and B. De Strooper. 2001. Interaction with telencephalin and the amyloid precursor protein predicts a ring structure for presenilins. *Neuron.* 32:579–589.

Botelho, R.J., M. Teruel, R. Dierckman, R. Anderson, A. Wells, J.D. York, T. Meyer, and S. Grinstein. 2000. Localized biphasic changes in phosphatidylinositol-4,5-bisphosphate at sites of phagocytosis. *J. Cell Biol.* 151:1353–1368.

Cai, D., J.Y. Leem, J.P. Greenfield, P. Wang, B.S. Kim, R. Wang, K.O. Lopes, S.H. Kim, H. Zheng, P. Greengard, et al. 2003. Presenilin-1 regulates intracellular trafficking and cell surface delivery of β-amyloid precursor protein. *J. Biol. Chem.* 278:3446–3454.

Cataldo, A.M., J.L. Barnett, C. Pieroni, and R.A. Nixon. 1997. Increased neuronal endocytosis and protease delivery to early endosomes in sporadic Alzheimer's disease: neuropathologic evidence for a mechanism of increased β-amyloidogenesis. *J. Neurosci.* 17:6142–6151.

Cupers, P., M. Bentahir, K. Craessaerts, I. Orlans, H. Vanderstichele, P. Saftig, B. De Strooper, and W. Annaert. 2001. The discrepancy between presenilin subcellular localization and γ-secretase processing of amyloid precursor protein. *J. Cell Biol.* 154:731–740.

De Strooper, B. 2003. Aph-1, Pen-2, and Nicastrin with Presenilin generate an active γ-secretase complex. *Neuron.* 38:9–12.

De Strooper, B., P. Saftig, K. Craessaerts, H. Vanderstichele, G. Guhde, W. Annaert, K. Von Figura, and F. Van Leuven. 1998. Deficiency of presenilin-1 inhibits the normal cleavage of amyloid precursor protein. *Nature.* 391:387–390.

Eskelinen, E.L. 2004. Macroautophagy in mammalian cells. *In* Lysosomes. P. Saftig, editor. Landes Bioscience, Georgetown, TX. 1–15.

Eskelinen, E.L., A.L. Illert, Y. Tanaka, G. Schwarzmann, J. Blanz, K. Von Figura, and P. Saftig. 2002. Role of LAMP-2 in lysosome biogenesis and autophagy. *Mol. Biol. Cell.* 13:3355–3368.

Gahmberg, C.G. 1997. Leukocyte adhesion: CD11/CD18 integrins and intercellular adhesion molecules. *Curr. Opin. Cell Biol.* 9:643–650.

Goslin, K., and G.A. Banker. 1991. Rat hippocampal neurons in low density culture. *In* Culturing Nerve Cells. K. Goslin, editor. MIT Press, Cambridge, MA. 251–281.

Greenberg, S., and S. Grinstein. 2002. Phagocytosis and innate immunity. *Curr.*

Opin. Immunol. 14:136–145.

Jellinger, K.A., and C. Stadelmann. 2000. Mechanisms of cell death in neurodegenerative disorders. *J. Neural Transm. Suppl.* 59:95–114.

Kabeya, Y., N. Mizushima, T. Ueno, A. Yamamoto, T. Kirisako, T. Noda, E. Kominami, Y. Ohsumi, and T. Yoshimori. 2000. LC3, a mammalian homologue of yeast Apg8p, is localized in autophagosome membranes after processing. *EMBO J.* 19:5720–5728.

Kaether, C., S. Lammich, D. Edbauer, M. Ertl, J. Rietdorf, A. Capell, H. Steiner, and C. Haass. 2002. Presenilin-1 affects trafficking and processing of βAPP and is targeted in a complex with nicastrin to the plasma membrane. *J. Cell Biol.* 158:551–561.

Kang, D.E., S. Soriano, X. Xia, C.G. Eberhart, B. De Strooper, H. Zheng, and E.H. Koo. 2002. Presenilin couples the paired phosphorylation of β-catenin independent of axin: implications for β-catenin activation in tumorigenesis. *Cell.* 110:751–762.

Kegel, K.B., M. Kim, E. Sapp, C. McIntyre, J.G. Castano, N. Aronin, and M. DiFiglia. 2000. Huntingtin expression stimulates endosomal-lysosomal activity, endosome tubulation, and autophagy. *J. Neurosci.* 20:7268–7278.

Koike, M., H. Nakanishi, P. Saftig, J. Ezaki, K. Isahara, Y. Ohsawa, W. Schulz-Schaeffer, T. Watanabe, S. Waguri, S. Kametaka, et al. 2000. Cathepsin D deficiency induces lysosomal storage with ceroid lipofuscin in mouse CNS neurons. *J. Neurosci.* 20:6898–6906.

Koster, A.J., and J. Klumperman. 2003. Electron microscopy in cell biology: integrating structure and function. *Nat. Rev. Mol. Cell. Biol.* 4Suppl:SS6–SS10.

Larsen, K.E., and D. Sulzer. 2002. Autophagy in neurons: a review. *Histol. Histopathol.* 17:897–908.

Maltese, W.A., S. Wilson, Y. Tan, S. Suomensaari, S. Sinha, R. Barbour, and L. McConlogue. 2001. Retention of the Alzheimer's amyloid precursor fragment C99 in the endoplasmic reticulum prevents formation of amyloid β-peptide. *J. Biol. Chem.* 276:20267–20279.

Mathews, P.M., C.B. Guerra, Y. Jiang, O.M. Grbovic, B.H. Kao, S.D. Schmidt, R. Dinakar, M. Mercken, A. Hille-Rehfeld, J. Rohrer, et al. 2002. Alzheimer's disease-related overexpression of the cation-dependent mannose 6-phosphate receptor increases Aβ secretion: role for altered lysosomal hydrolase distribution in β-amyloidogenesis. *J. Biol. Chem.* 277:5299–5307.

May, R.C., and L.M. Machesky. 2001. Phagocytosis and the actin cytoskeleton. *J. Cell Sci.* 114:1061–1077.

Michiels, F., H. van Es, L. van Rompaey, P. Merchiers, B. Francken, K. Pittois, J. van der Schueren, R. Brys, J. Vandersmissen, F. Beirinckx, et al. 2002. Arrayed adenoviral expression libraries for functional screening. *Nat. Biotechnol.* 20:1154–1157.

Mizushima, N., A. Yamamoto, M. Hatano, Y. Kobayashi, Y. Kabeya, K. Suzuki, T. Tokuhisa, Y. Ohsumi, and T. Yoshimori. 2001. Dissection of autophagosome formation using Apg5-deficient mouse embryonic stem cells. *J. Cell Biol.* 152:657–668.

Mizushima, N., Y. Ohsumi, and T. Yoshimori. 2002. Autophagosome formation in mammalian cells. *Cell Struct. Funct.* 27:421–429.

Munafo, D.B., and M.I. Colombo. 2001. A novel assay to study autophagy: regulation of autophagosome vacuole size by amino acid deprivation. *J. Cell Sci.* 114:3619–3629.

Nakamura, K., T. Manabe, M. Watanabe, T. Mamiya, R. Ichikawa, Y. Kiyama, M. Sanbo, T. Yagi, Y. Inoue, T. Nabeshima, et al. 2001. Enhancement of hippocampal LTP, reference memory and sensorimotor gating in mutant mice lacking a telencephalon-specific cell adhesion molecule. *Eur. J. Neurosci.* 13:179–189.

Naruse, S., G. Thinakaran, J.J. Luo, J.W. Kusiak, T. Tomita, T. Iwatsubo, X. Qian, D.D. Ginty, D.L. Price, D.R. Borchelt, et al. 1998. Effects of PS1 deficiency on membrane protein trafficking in neurons. *Neuron.* 21:1213–1221.

Nyabi, O., M. Bentahir, K. Horre, A. Herreman, N. Gottardi-Littell, C. Van Broeckhoven, P. Merchiers, K. Spittaels, W. Annaert, and B. De Strooper. 2003. Presenilins mutated at Asp-257 or Asp-385 restore Pen-2 expression and Nicastrin glycosylation but remain catalytically inactive in the absence of wild type Presenilin. *J. Biol. Chem.* 278:43430–43436.

Oorschot, V., H. De Wit, W.G. Annaert, and J. Klumperman. 2002. A novel flat-embedding method to prepare ultrathin cryosections from cultured cells in their in situ orientation. *J. Histochem. Cytochem.* 50:1067–1080.

Pasternak, S.H., R.D. Bagshaw, M. Guiral, S. Zhang, C.A. Ackerley, B.J. Pak, J.W. Callahan, and D.J. Mahuran. 2003. Presenilin-1, nicastrin, amyloid precursor protein, and γ-secretase activity are co-localized in the lysosomal membrane. *J. Biol. Chem.* 278:26687–26694.

Qian, S., P. Jiang, X.M. Guan, G. Singh, M.E. Trumbauer, H. Yu, H.Y. Chen, L.H. Van de Ploeg, and H. Zheng. 1998. Mutant human presenilin 1 protects presenilin 1 null mouse against embryonic lethality and elevates Aβ1-42/43 expression. *Neuron.* 20:611–617.

Rechards, M., W. Xia, V.M. Oorschot, D.J. Selkoe, and J. Klumperman. 2003. Presenilin-1 exists in both pre- and post-Golgi compartments and recycles via COPI-coated membranes. *Traffic.* 4:553–565.

Selkoe, D., and R. Kopan. 2003. Notch and Presenilin: regulated intramembrane proteolysis links development and degeneration. *Annu. Rev. Neurosci.* 26: 565–597.

Slot, J.W., H.J. Geuze, S. Gigengack, G.E. Lienhard, and D.E. James. 1991. Immuno-localization of the insulin regulatable glucose transporter in brown adipose tissue of the rat. *J. Cell Biol.* 113:123–135.

Struhl, G., and A. Adachi. 2000. Requirements for presenilin-dependent cleavage of notch and other transmembrane proteins. *Mol. Cell.* 6:625–636.

Tanaka, Y., G. Guhde, A. Suter, E.L. Eskelinen, D. Hartmann, R. Lullmann-Rauch, P.M. Janssen, J. Blanz, K. von Figura, and P. Saftig. 2000. Accumulation of autophagic vacuoles and cardiomyopathy in LAMP-2-deficient mice. *Nature.* 406:902–906.

Tian, L., H. Nyman, P. Kilgannon, Y. Yoshihara, K. Mori, L.C. Andersson, S. Kaukinen, H. Rauvala, W.M. Gallatin, and C.G. Gahmberg. 2000. Intercellular adhesion molecule-5 induces dendritic outgrowth by homophilic adhesion. *J. Cell Biol.* 150:243–252.

Wilson, C.A., D.D. Murphy, B.I. Giasson, B. Zhang, J.Q. Trojanowski, and V.M. Lee. 2004. Degradative organelles containing mislocalized α- and β-synuclein proliferate in presenilin-1 null neurons. *J. Cell Biol.* 165:335–346.

Wolfe, M.S., W. Xia, B.L. Ostaszewski, T.S. Diehl, W.T. Kimberly, and D.J. Selkoe. 1999. Two transmembrane aspartates in presenilin-1 required for presenilin endoproteolysis and γ-secretase activity. *Nature.* 398:513–517.

Yamamoto, A., Y. Tagawa, T. Yoshimori, Y. Moriyama, R. Masaki, and Y. Tashiro. 1998. Bafilomycin A1 prevents maturation of autophagic vacuoles by inhibiting fusion between autophagosomes and lysosomes in rat hepatoma cell line, H-4-II-E cells. *Cell Struct. Funct.* 23:33–42.

Yoo, A.S., I. Cheng, S. Chung, T.Z. Grenfell, H. Lee, E. Pack-Chung, M. Handler, J. Shen, W. Xia, G. Tesco, et al. 2000. Presenilin-mediated modulation of capacitative calcium entry. *Neuron.* 27:561–572.

Yoshihara, Y., S. Oka, Y. Nemoto, Y. Watanabe, S. Nagata, H. Kagamiyama, and K. Mori. 1994. An ICAM-related neuronal glycoprotein, telencephalin, with brain segment-specific expression. *Neuron.* 12:541–553.